RESEARCH ARTICLE | JULY 27 2016

Micro-CT at the imaging beamline P05 at PETRA III FREE

Fabian Wilde; Malte Ogurreck; Imke Greving; Jörg U. Hammel; Felix Beckmann; Alexander Hipp; Lars Lottermoser; Igor Khokhriakov; Pavel Lytaev; Thomas Dose; Hilmar Burmester; Martin Müller; Andreas Schreyer

AIP Conf. Proc. 1741, 030035 (2016)
https://doi.org/10.1063/1.4952858

Micro-CT at the Imaging Beamline P05 at PETRA III

Fabian Wilde[1,a)], Malte Ogurreck[1], Imke Greving[1], Jörg U. Hammel[1], Felix Beckmann[1], Alexander Hipp[1], Lars Lottermoser[1], Igor Khokhriakov[1], Pavel Lytaev[1], Thomas Dose[1], Hilmar Burmester[1], Martin Müller[1] and Andreas Schreyer[1]

[1]*Helmholtz-Zentrum Geesthacht, Max-Planck-Straße 1, 21502 Geesthacht*

[a)]Corresponding author: fabian.wilde@hzg.de

Abstract. The Imaging Beamline (IBL) P05 is operated by the Helmholtz-Zentrum Geesthacht and located at the DESY storage ring PETRA III. IBL is dedicated to X-ray full field imaging and consists of two experimental end stations. A micro tomography end station equipped for spatial resolutions down to 1 µm and a nano tomography end station for spatial resolutions down to 100 nm. The micro tomography end station is in user operation since 2013 and offers imaging with absorption contrast, phase enhanced absorption contrast and phase contrast methods. We report here on the current status and developments of the micro tomography end station including technical descriptions and show examples of research performed at P05.

INTRODUCTION

Since the uptake of full user operation 2013, the main focus of the micro tomography experiment of the Imaging Beamline P05 was on providing high quality, absorption contrast tomograms with very high density resolution. Since this kind of tomograms were already successfully delivered by the now discontinued DORIS beamlines W2 and BW2 providing a large user base, a continuation of this practice was paramount. Now in addition to the absorption contrast technique, propagation based phase contrast can be offered to users and the overall reliability of the experiment continually increases. A next step in the experimental evolution focuses on speeding up the scan process and offer more phase contrast methods with better performance.

BEAMLINE DESCRIPTION

The Imaging Beamline P05 is located in a low-β section of the PETRA III storage ring. The insertion device is a 2 m U29 undulator, canted by 5 mrad to the P06 undulator, which is located downstream. As shown in figure 1, the front-end furthermore contains a slit system and filters (4 mm glassy carbon and 300 µm CVD with 50 µm Cu) [1]. Two monochromators are located in the optics hutch: a Double Crystal Monochromator (DCM) and a Double Multilayer Monochromator (DMM). The DCM is designed by DESY and built by Oxford Instruments with Si [111] and Si [311] crystal pairs in Bragg geometry and a energy independent vertical offset between 20–24 mm. The DMM is built by Bruker and contains three sets of multilayers. Both monochromators are independently cooled with liquid nitrogen. While the DCM delivers a highly monochromatic beam ($\Delta E/E \approx 10^{-4}$), the DMM will provide an energetically broader beam ($\Delta E/E \approx 10^{-2}$) thus yielding much higher flux on the sample. The DMM is already installed in the beamline, but not yet in operation. It is expected that first experiments with the DMM can be performed later this year. The accessible energy of P05 ranges between 5–50 keV and is equipped with 3 multilayer sets for different energies. The ring vacuum and and beamline vacuum section are separated by a water cooled diamond window in front of the monochromators. An in-vacuum slit system is installed right behind the DCM. Furthermore the optics hutch contains a vacuum chamber at the end of the optics hutch which can be equipped with lenses, slits and beam diagnostic elements like diodes. The beam then passes through the first experimental hutch in an evacuated tube until at 85.9 m from the source another diamond window releases the x-ray beam into air. The sample is hit at 86.5 m from the source. The most important beamline parameters are listed in table 1.

Proceedings of the 12th International Conference on Synchrotron Radiation Instrumentation – SRI2015
AIP Conf. Proc. 1741, 030035-1–030035-4; doi: 10.1063/1.4952858
Published by AIP Publishing. 978-0-7354-1398-6/$30.00

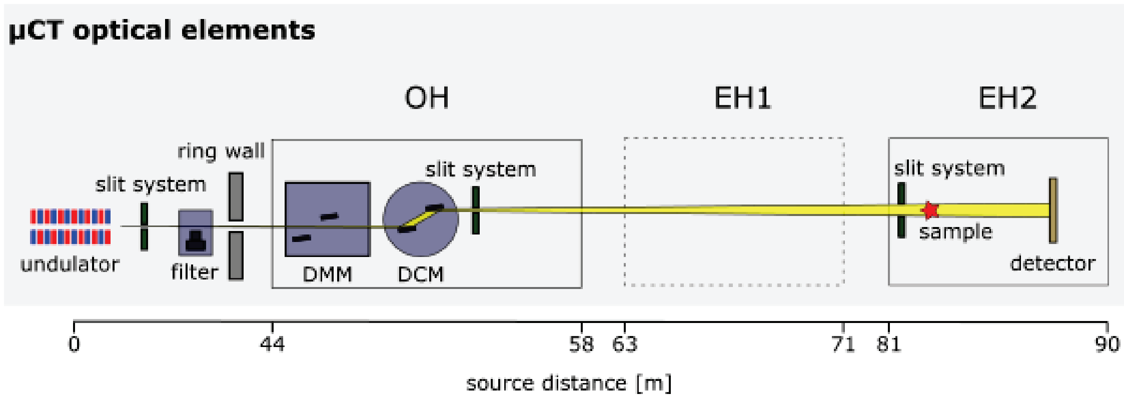

FIGURE 1. Sketch of the P05 beamline. The beamline consists of the front-end containing the undulator, slits and filters, an optics hutch (OH) with a double crystal monochromator and a double multilayer monochromator, the first experimental hutch (EH1) used for nano tomography and the second experimental hutch (EH2) for microtomographic use.

TABLE 1. General P05 Beamline parameters.

Energy range	5–50 keV
Insertion device	U29 Undulator in low-β section
Source size	36 µm × 6.1 µm (at 10 keV)
Source divergence	28 µrad × 4.0 µrad (at 10 keV)
Filters	4 mm glassy carbon and 300 µm CVD with 50 µm Cu
Monochromators	Double Crystal Monochromator, Si [111]/[311] in Bragg geometry ($\Delta E/E \approx 10^{-4}$), Double Multilayer Monochromator with three different ML pairs ($\Delta E/E \approx 10^{-2}$)

MICRO TOMOGRAPHY SETUP

The micro tomography setup of P05 is shown in Figure 2. The coordinate system of this setup is shown in the lower left corner of figure 2a. Rotations around the axis (x, y, z) are denoted in the following as: $x \Rightarrow \omega$, $y \Rightarrow \phi$, $z \Rightarrow \kappa$ The mechanical setup is composed of four stages:

1. a massive granite base stage mounted on a tripod (built inhouse by HZG Technikum) $(x, z, \omega, \phi, \kappa)$
2. a high precision, air bearing rotation stage (Aerotech ABRT 260) mounted on a tripod $(x, z, \omega, \phi, \kappa)$
3. a camera stage on a air bearing linear translation mounted on a tripod (PImiCos) (y, z, ω, ϕ)
4. a piezo controlled sample stage mounted inside the rotation stage for sample alignment (Attocube) (x, y, z, ω, ϕ)

The rotation stage is surrounded by roller bearing rotation stage (Aerotech ALAR 325 LP) which rotates synchronous and carries a slip ring for the electrical connectors of the piezo sample stage. This construction allows for endless rotation with highest precision while still supplying electrical connection to the integrated sample stage. Each tripod substructure is able to move with 1 µm precision allowing for very precise alignment of the setup. A $CdWO_4$ single crystal scintillator of 100 µm thickness converts the x-ray to visible light. The sample to scintillator distance can be varied within 0–1480 mm. A sketch of the microscope optics is shown in figure 2b. The microscope optics is custom designed and built by POG (Präzisionsoptik Gera). Behind the scintillator a mirror is mounted to prevent the objective lens being in the direct x-ray beam path thus reducing radiation damage. With four tubus objectives mounted on a revolver it is possible to switch between four different magnification settings, cf. table 2. Focal lengths are subsequently adjusted by the camera distance in the following camera housing depicted in figure 2c. The camera housing holds up to two cameras. The optical path can be switched between the two cameras with a fast moving mirror. Currently, just one CCD camera is installed: a EHD SC09000M CCD camera with 3056×3056 pixels and 12 µm pixel size. Optionally, either two different cameras (e.g a CCD and and fast CMOS camera) can be operated without the necessity of physically mounting a camera, or two identical CCD cameras with higher readout times can be mounted.

In the latter configuration, the overall scanning process can be sped up by exposing one of the two cameras while reading out the other out. With this technique we estimate to achieve scan times around 15 minutes while maintaining

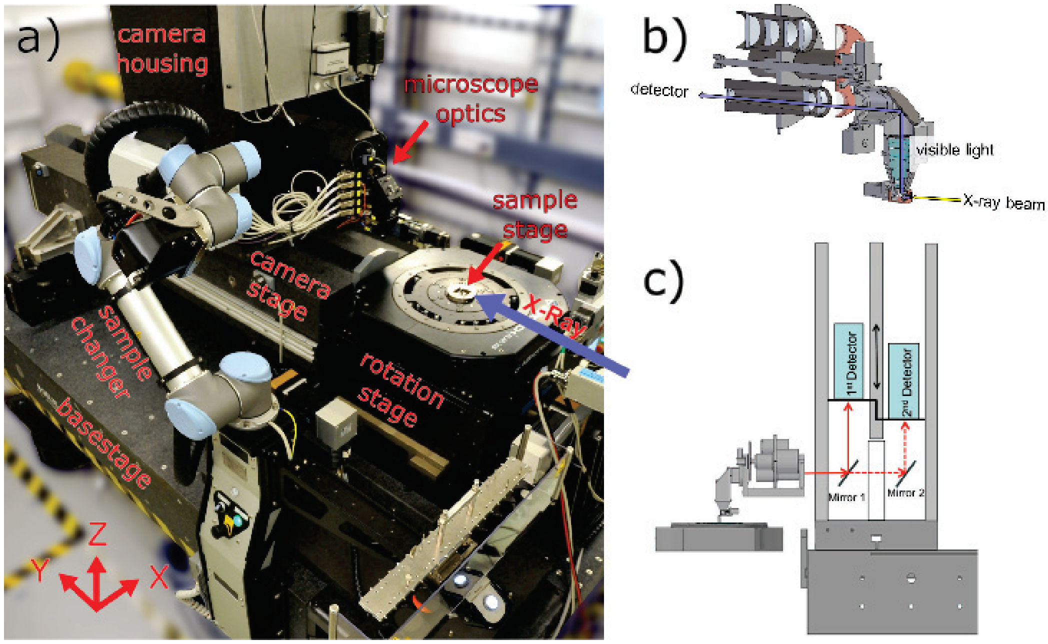

FIGURE 2. a) the basic micro tomography setup consists of four spatial motion stages (base stage , rotation stage, camera stage and sample stage) and a microscope system including two cameras. Also visible in this photo is the sample changer and a slit system. **b)** sketch of the microscope optics. Note that the objective lens is not in the x-ray beam path. **c)** the camera housing offers space for two cameras. Mirror 1 is mounted on a fast linear stage to allow for switching the optical path to the 2nd camera.

very high density resolution. The micro CT setup is equipped with a sample changer, that can change up to 20 samples without manual interference.

TABLE 2. Visible light optical parameters of the microscope system at P05 in combination with an EHD SC09000M CCD (3056 × 3056 pixel with 12 µm pixel size). Note that for lower FOVs the beam spot size at the sample position of $7 \times 2\text{mm}^2$ may vertically limit the usable FOV.

Magnification	**FOV**	**Pixel edge length**	**Spatial Resolution**
5×	7.3×7.3 mm^2	2.4 µm	2.4 µm
10×	3.6×3.6 mm^2	1.2 µm	1.2 µm
20×	1.8×1.8 mm^2	0.6 µm	1 µm*
40×	0.9×0.9 mm^2	0.3 µm	1 µm*

* Determined by measuring structural sizes (e.g. cracks, pores and small particles) in reconstructed data.

Several different imaging methods have been successfully performed at the micro CT end station: high density-resolution absorption tomography, grating-based phase contrast [2] and propagation-based phase-contrast tomography. The scientific topics covered in user experiments so far include materials science, medicine, biology and geology first published examples are e.g. the investigation of the ageing of an exhaust gas catalyst [3] and the analysis of the head morphology of a silverfish [4]. Due to generous space around the sample extended sample environments can easily be implemented. First successful experiments using furnaces, load frames, cryo streams and fluid chambers were already performed.

A good example for the high quality of the absorption contrast method at the P05 micro tomography end station is shown in figure 3. The insect investigated here is a moss flea (*Caurinus sp.* with a length of roughly 2 mm. The aim of the investigation was to resolve phylogenetic relationships in the insect tree of life by studying morphological characters. For this kind of research the data often needs to be segmented. Since soft tissue parts in the insect are very small a very high density resolution is needed for identification and segmentation of anatomical structures.

FIGURE 3. Cross section in a volume rendering of a moss flea (*Caurinus sp.*). The tomogram was taken at an energy of 8 keV using the 20× magnification (see table 2). In order to enhance the density resolution, a 2× binning was applied to the radiograms yielding a spatial resolution of 1.2 µm.

CONCLUSIONS

The micro tomography end station of the Imaging Beamline P05 at PETRA III is very well suited for a wide range of scientific topics. Special emphasis is currently on the generation of high quality absorption contrast tomograms. Grating based phase contrast and propagation based phase contrast methods have already been successfully applied at P05 and are now part of the regular user operation. With an low failure rate of the experimental setup and the use of the sample changer an appropriately high throughput can be realized. Use of sample environments is generally easy and encouraged. Apart for improvement of the current experimental setup the next steps will be to implement high speed tomography. A standard high speed tomogram will thus be acquired in a few minutes.

ACKNOWLEDGMENTS

We would like to thank F. Friedrich of the University of Hamburg for his study on the moss flea and all our users for feedback, suggestions and active improvements of the setup. Furthermore we thank all support groups of DESY and HZG for their extensive help. A special thanks to the former beamline group members Astrid Haibel who was initially responsible for the beamline and Julia Herzen whose immense work helped shape the experiment to its current state. M. Ogurreck gratefully acknowledges financial support from the German Research Foundation (DFG) via SFB 986 Tailor-Made multiscale materials – M^3, project Z2.

REFERENCES

[1] H. Schulte-Schrepping, M. Degenhardt, H.-B. Peters, U. Hahn, J. Heuer, and M. Hesse, Journal of Physics: Conference Series **425**, p. 042005 (2013).

[2] A. Hipp, F. Beckmann, P. Lytaev, I. Greving, L. Lottermoser, T. Dose, R. Kirchhof, H. Burmester, A. Schreyer, and J. Herzen, "Grating-based x-ray phase-contrast imaging at PETRA III," in *Proc. SPIE 9212, Developments in X-Ray Tomography IX*, edited by S. R. Stock.

[3] G. Hofmann, A. Rochet, S. Baier, M. Casapu, S. Ritter, F. Wilde, M. Ogurreck, F. Beckmann, and J.-D. Grunwaldt, Journal of Physics: Conference Series **499**, p. 012017 (2014).

[4] A. Blanke, M. Koch, B. Wipfler, F. Wilde, and B. Misof, Frontiers in Zoology **11**, p. 16 (2014).

[5] I. Greving, F. Wilde, M. Ogurreck, J. Herzen, J. U. Hammel, A. Hipp, F. Friedrich, L. Lottermoser, T. Dose, H. Burmester, M. Müller, and F. Beckmann, "P05 imaging beamline at PETRA III: first results," in *Developments in X-Ray Tomography IX*, Proc. SPIE, edited by S. R. Stock (2014), pp. 92120O–92120O–8.

[6] A. Haibel, F. Beckmann, T. Dose, J. Herzen, M. Ogurreck, M. Müller, and A. Schreyer, Powder Diffraction **25**, 161–164 (2010).

[7] M. Ogurreck, F. Wilde, J. Herzen, F. Beckmann, V. Nazmov, J. Mohr, A. Haibel, M. Müller, and A. Schreyer, Journal of Physics: Conference Series **425**, p. 182002 (2013).